Scilight

Bioelectrochemistry and Biosensors

https://www.sciltp.com/journals/bebs

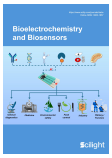

Article

Check for updates

Metal Nanoparticle-Based Amperometric Biosensors for Ethanol Determination: Comparative Study of Alcohol Oxidase and Alcohol Dehydrogenase Bioelectrodes

Nataliya Stasyuk [1,2,*], Olha Demkiv [1,2], Taras Kavetskyy [3,4,5,6], Halyna Klepach [4], Jolita Ostrauskaite [7] and Mykhailo Gonchar [1,4]

[1] Institute of Cell Biology, National Academy of Sciences of Ukraine, 79005 Lviv, Ukraine
[2] Institute of Physical Chemistry, Polish Academy of Sciences, 01-224 Warsaw, Poland
[3] Department of Physics and Information Systems, Drohobych Ivan Franko State Pedagogical University, 82100 Drohobych, Ukraine
[4] Department of Biology and Chemistry, Drohobych Ivan Franko State Pedagogical University, 82100 Drohobych, Ukraine
[5] Department of Innovative Technologies and Teaching Methods of Natural Sciences, South Ukrainian National Pedagogical University Named after K.D. Ushynsky, 65020 Odesa, Ukraine
[6] Institute of Physics, Slovak Academy of Sciences, 84511 Bratislava, Slovakia
[7] Department of Polymer Chemistry and Technology, Kaunas University of Technology, 50254 Kaunas, Lithuania
* Correspondence: stasuk_natalia@ukr.net

How To Cite: Stasyuk, N.; Demkiv, O.; Kavetskyy, T.; et al. Metal Nanoparticle-Based Amperometric Biosensors for Ethanol Determination: Comparative Study of Alcohol Oxidase and Alcohol Dehydrogenase Bioelectrodes. *Bioelectrochemistry and Biosensors* **2026**, *1*(1), 8. https://doi.org/10.53941/bebs.2026.100008

Received: 30 June 2026
Revised: 24 July 2026
Accepted: 29 July 2026
Published: 31 July 2026

Abstract: Rapid and reliable determination of ethanol is important in food quality control, clinical diagnostics, and industrial monitoring. In this work, amperometric biosensors based on alcohol oxidase (AO) and alcohol dehydrogenase (ADH) were developed and compared for ethanol determination. Copper (nCu) and bimetallic copper–gold (nCuAu) nanoparticles were synthesized by chemical reduction and characterized as nanozyme-like electrocatalytic materials. The catalytic activity of the nanoparticles toward hydrogen peroxide reduction was investigated and applied for the construction of AO-based biosensors. Several enzyme immobilization approaches, including glutaraldehyde vapor crosslinking, dialysis membrane entrapment, and polymer matrices (ELO, ELO/RD1, and M1-2), were evaluated. The ELO matrix provided efficient immobilization while preserving catalytic activity and was selected for further studies. Among AO-based bioelectrodes, AO/nCu/GE exhibited higher sensitivity toward ethanol than AO/nCuAu/GE. In parallel, an ADH-based biosensor incorporating $NADP^+$ and benzoquinone as an electron-transfer mediator was developed. The ADH/ELO/GE biosensor demonstrated the highest sensitivity (305 $A \cdot M^{-1} \cdot m^{-2}$), a low detection limit (0.005 mM), good reproducibility (RSD = 3.5%), and acceptable storage stability. The biosensor showed negligible interference from common electroactive compounds and was successfully validated for ethanol determination in commercial wine samples. The results demonstrate the potential of enzyme–nanozyme hybrid systems as effective analytical platforms for ethanol monitoring.

Keywords: ethanol biosensor; alcohol oxidase; alcohol dehydrogenase; nanozyme; copper nanoparticles; gold–copper nanoparticles; amperometric biosensor

1. Introduction

Ethanol is one of the most widely monitored analytes in food quality control, clinical diagnostics, biofuel production, and industrial fermentation processes. Conventional analytical methods such as gas chromatography

Copyright: © 2026 by the authors. This is an open access article under the terms and conditions of the Creative Commons Attribution (CC BY) license (https://creativecommons.org/licenses/by/4.0/).
Publisher's Note: Scilight stays neutral with regard to jurisdictional claims in published maps and institutional affiliations.

and spectrophotometry provide high accuracy but require expensive instrumentation, trained personnel, and time-consuming sample preparation, limiting their use for rapid or on-site analysis. Electrochemical biosensors offer a powerful alternative due to their simplicity, high sensitivity, portability, and compatibility with miniaturized devices. Enzyme-based biosensors remain the most widely used class of analytical devices because of their high selectivity and catalytic efficiency [1,2].

Alcohol oxidase (AO) and alcohol dehydrogenase (ADH) are the two most commonly employed enzymes for ethanol biosensing. AO catalyzes ethanol oxidation with oxygen as an electron acceptor, producing acetaldehyde and hydrogen peroxide, which can be directly detected electrochemically. ADH relies on NAD^+/NADH cofactors and typically requires a redox mediator for efficient electron transfer, resulting in higher sensitivity but more complex electrode architecture [3,4].

Recent advances in biosensor engineering have demonstrated that immobilization matrices and electron-transfer mediators play a crucial role in performance optimization of dehydrogenase-based systems. Polymer matrices can significantly influence enzyme stability, diffusion properties, and apparent kinetic parameters [4,5]. In parallel, nanomaterials have become central components in modern biosensor design. Metal nanoparticles exhibit high conductivity and catalytic activity [6]. In particular, Cu-based nanostructures exhibit intrinsic peroxidase-like (nanozyme) activity, which can be exploited for signal amplification in oxidase-based biosensors [7].

The concept of nanozyme-assisted biosensing has emerged as a promising strategy to improve sensitivity and operational stability. However, the integration of nanozymes with enzymatic systems remains challenging because enzyme–nanoparticle interactions and local microenvironment effects strongly influence overall catalytic efficiency and signal output [8]. Recent progress in electrochemical biosensors has also highlighted significant advances in ethanol detection for food and beverage analysis, including wine, beer, and fermentation systems, where selectivity and stability remain key challenges [9].

Despite this progress, three major challenges remain unresolved: (i) lack of systematic comparison between AO- and ADH-based ethanol biosensors under identical nanomaterial platforms; (ii) insufficient understanding of nCu vs. nCuAu nanozyme contributions in enzymatic signal transduction; and (iii) limited optimization of immobilization matrices balancing enzyme activity and mass transport.

In this work, we address these challenges by developing and comparing nCu and nCuAu nanoparticle-based amperometric biosensors for ethanol detection integrated with AO and ADH enzymatic systems. The study systematically evaluates the role of nanozyme composition and polymer immobilization matrices (ELO, ELO/RD1, M1-2) in determining analytical performance. The results provide mechanistic insight into enzyme–nanozyme synergy and establish design principles for next-generation ethanol biosensors.

2. Materials and Methods

2.1. Synthesis of Polymer Immobilization Matrices

Polymer immobilization matrices were marked as ELO—epoxidized linseed oil (ELO) with 3 mol.% of photoinitiator (PI) (triarylsulfonium hexafluoroantimonate salts, TAS), ELO/RD1—epoxidized linseed oil (ELO) with 10 mol.% of trimethylolpropane triglycidyl ether (RD1) and 3 mol.% of PI (TAS), and M1-2—mixture of acrylated epoxidized soybean oil (AESO) and vanillin dimethacrylate (VDM) (molar ratio of monomers 1:0.5) with 3 mol.% of PI (2,2-dimethoxy-2-phenylacetophenone, DMPA). The initial mixtures of above mentioned compositions ELO, ELO/RD1 and M1-2 were stirred at 25 °C for 5 min until reached the homogeneous consistency. The homogenous mixtures of resins were then poured into Teflon mold (3 × 15 mm) and cured for 3–5 min under a 500 W Helios Italquartz GR.E UV lamp emitting light at a wavelength of 250–450 nm and an intensity of 310 mW cm^{-2} for several min until a solid polymer was formed.

2.2. Synthesis of Metallic Nanoparticles

Copper (nCu) and bimetallic copper–gold (nCuAu) nanoparticles were synthesized by chemical reduction of $CuSO_4$ and $HAuCl_4$ solutions using sodium borohydride as a reducing agent in the presence of cetyltrimethylammonium bromide (CTAB). The nanoparticles were obtained by mixing precursor salt solutions followed by reduction with 1 mM $NaBH_4$ in the presence of 1 mM CTAB.

2.3. Fabrication of Nanozyme-Modified Electrodes

Graphite rod electrodes (GE) were modified with synthesized nanoparticles. Their electrocatalytic activity toward hydrogen peroxide reduction was evaluated by chronoamperometry in 50 mM phosphate buffer (pH 7.5) at an applied potential of −200 mV versus Ag/AgCl (3M KCl).

2.4. Construction of Alcohol Oxidase Biosensors

Alcohol oxidase (160 U·mL^{-1}) was immobilized onto nanozyme-modified graphite electrodes using several approaches:

(1) Glutaraldehyde vapor cross-linking;
(2) Dialysis membrane entrapment;
(3) Immobilization within ELO polymer matrix;
(4) Immobilization within ELO/RD1 polymer matrix;
(5) Immobilization within M1-2 polymer matrix.

The resulting bioelectrodes were washed with phosphate buffer (50 mM, pH 7.5) before measurements.

2.5. Construction of Alcohol Dehydrogenase Biosensors

ADH (30 U·mL^{-1}) and $NADP^+$ were co-immobilized within the ELO matrix on graphite electrodes. Benzoquinone was used as a redox mediator. Electrochemical measurements were performed in 50 mM phosphate buffer (pH 7.5) using cyclic voltammetry and chronoamperometry.

2.6. Electrochemical Measurements

Electrochemical experiments were performed using an electrochemical workstation (Autolab PGSTAT 10, ECO Chemie) and GPES 4.9 (General Purpose Electrochemical System) software (Metrohm Autolab, Utrecht, The Netherlands). Cyclic voltammetry and chronoamperometric experiments were performed using Ag/AgCl (3M KCl) as the reference electrode. Ethanol calibration curves were obtained by successive additions of standard ethanol solutions. Sensitivity, linear range, apparent Michaelis–Menten constant (K_M^{app}), and detection limit were calculated from calibration data. All electrochemical measurements were performed in triplicate (n = 3) using independently prepared electrodes. Calibration curves are presented as mean ± standard deviation (SD), and error bars represent the standard deviation of three independent measurements.

2.7. Selectivity, Reproducibility, Stability and Real Sample Analysis

Possible interference from ascorbic acid, uric acid, dopamine, glutathione, NaCl, and KCl was investigated. Sensor reproducibility was evaluated through repeated measurements of 1.3 mM ethanol. Storage stability was assessed during two weeks at 4 °C. Commercial “Isabella” red wine samples were analyzed using the standard addition method [10] and compared with results obtained using a commercial enzymatic assay kit.

3. Results and Discussion

3.1. Synthesis, Characterization, and Electrocatalytic Properties of Cu and CuAu Nanozymes

Copper (nCu) and bimetallic copper–gold (nCuAu) nanoparticles were synthesized through chemical reduction of the corresponding metal salts using sodium borohydride as a reducing agent in the presence of CTAB as a stabilizing agent. The obtained nanomaterials were investigated as potential nanozyme-like electrocatalysts for hydrogen peroxide reduction, which is a key step in the development of oxidase-based biosensors.

The morphology of the synthesized nanoparticles was studied by scanning electron microscopy (SEM) (Figure 1). SEM images revealed substantial differences between the two synthesized materials. The nCuAu nanoparticles were predominantly spherical and relatively uniform in size, with an average diameter of approximately 50 nm. In contrast, copper particles formed larger aggregates with dimensions ranging from 1 to 3 μm. The considerably smaller size and higher surface-to-volume ratio of nCuAu nanoparticles are expected to provide a larger number of accessible catalytic sites and enhanced electron-transfer properties.

To evaluate their catalytic activity, the nanoparticles were deposited onto graphite electrodes and tested toward electrochemical reduction of hydrogen peroxide using chronoamperometry at −200 mV versus Ag/AgCl (3M KCl). Hydrogen peroxide is the reaction product generated during alcohol oxidase-catalyzed oxidation of ethanol and therefore serves as an important analytical intermediate (Figure 2).

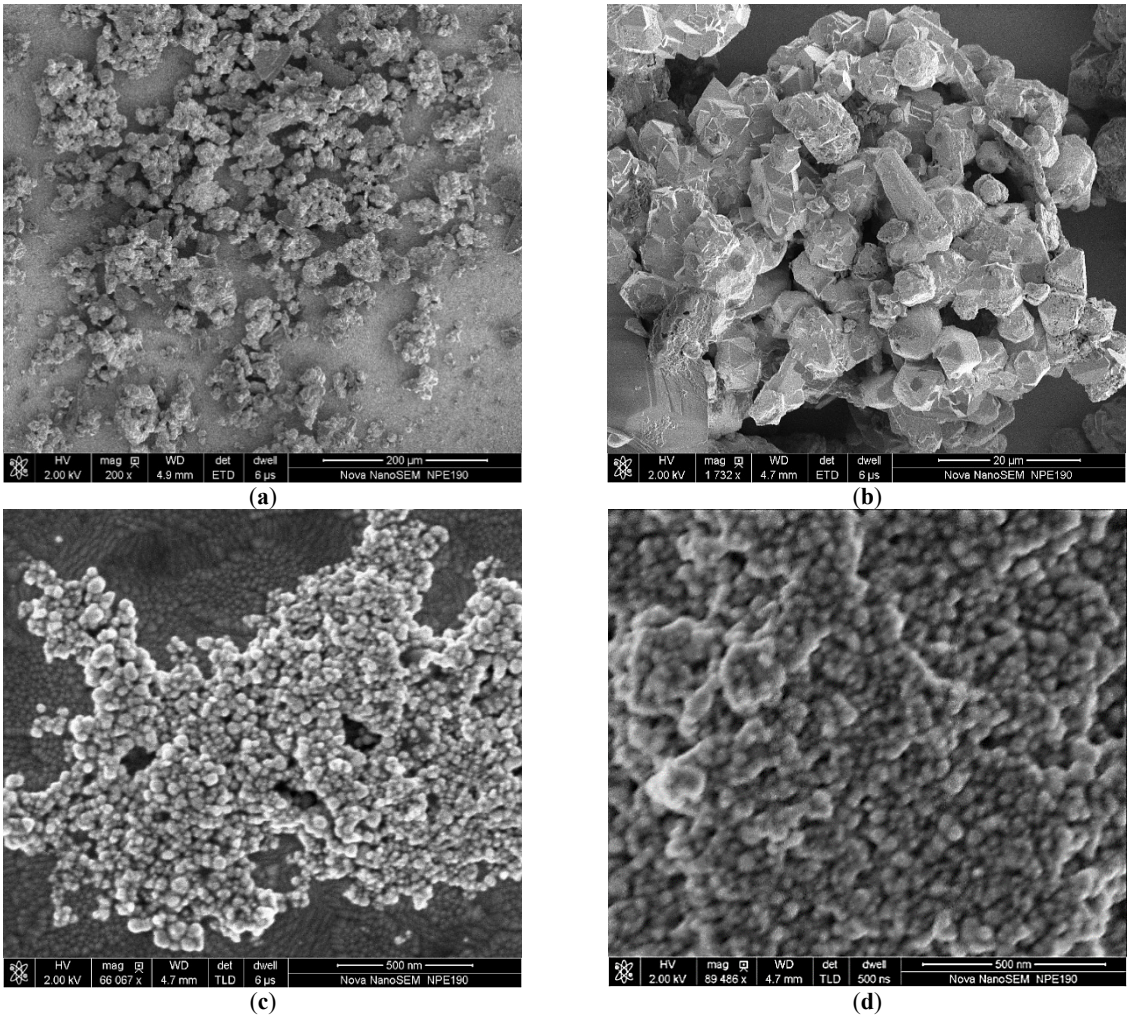

Figure 1. SEM micrographs showing the morphology of synthesized nanoparticles: nCu (**a**,**b**) and nAuCu (**c**,**d**) at different magnification.

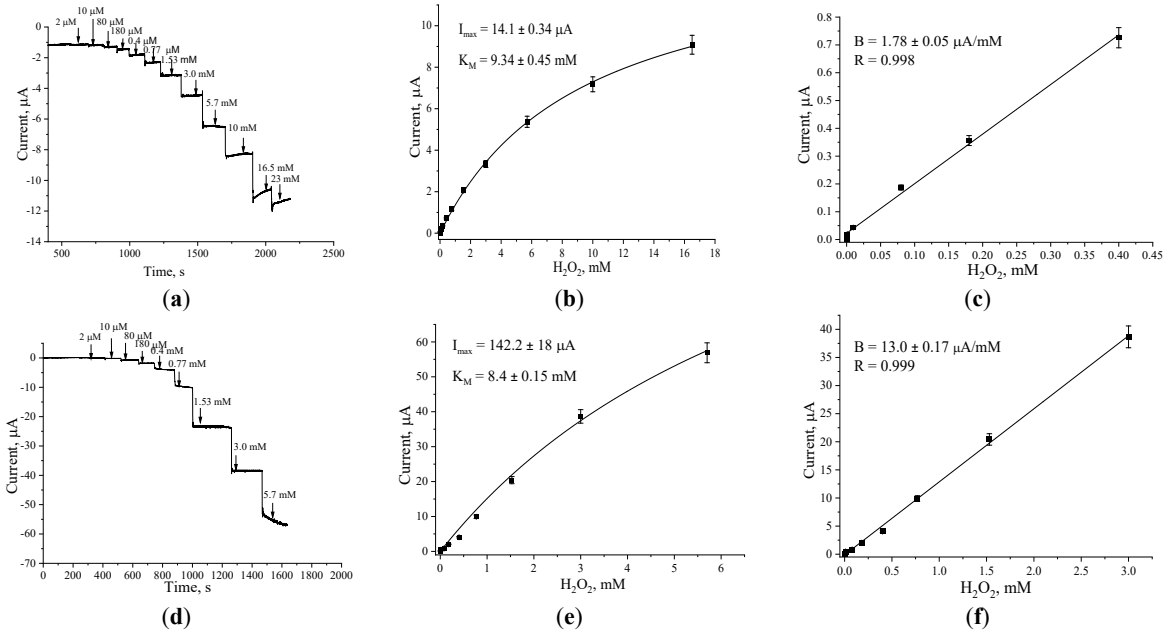

Figure 2. Electrochemical performance of nCu- and nCuAu-modified chemoelectrodes toward hydrogen peroxide detection. (**a**,**d**) Representative chronoamperometric responses; (**b**,**e**) dependence of steady-state current on H_2O_2 concentration; and (**c**,**f**) corresponding calibration curves in the linear concentration range for nCuAu (**a**–**c**) and nCu (**d**–**f**) electrodes. Measurements were performed at an applied potential of −200 mV vs. Ag/AgCl (3M KCl) in 50 mM phosphate buffer (pH 7.5) at 23 °C.

Both nanoparticle-modified electrodes exhibited catalytic activity toward hydrogen peroxide reduction; however, their analytical performance differed significantly. The nCuAu-modified electrode generated substantially higher current responses than the nCu-modified electrode over the investigated concentration range (Figure 2d–f). Analysis of calibration plots demonstrated that the sensitivity of the nCuAu electrode was approximately seven-fold higher than that of the nCu electrode (Figure 2a–c). This enhanced performance can be attributed to synergistic interactions between copper and gold atoms in the bimetallic structure, which facilitate electron transfer and improve catalytic efficiency.

The superior electrocatalytic properties of the nCuAu nanoparticles indicate that incorporation of gold into the copper matrix significantly enhances the catalytic reduction of hydrogen peroxide. Similar behavior has been reported for various bimetallic nanostructures, where electronic interactions between the constituent metals improve catalytic efficiency compared with their monometallic counterparts. These results confirm that both synthesized nanomaterials exhibit peroxidase-like (nanozyme) activity and are suitable platforms for the construction of oxidase-based amperometric biosensors. Accordingly, both nanozyme architectures were selected for integration with alcohol oxidase.

Interestingly, although the nCuAu nanozymes exhibited significantly higher electrocatalytic activity toward hydrogen peroxide reduction than nCu when evaluated as chemoelectrodes, this advantage was not reflected in the analytical performance of the corresponding alcohol oxidase-based biosensor. Instead, the AO/nCu/GE bioelectrode demonstrated substantially higher sensitivity toward ethanol. This finding suggests that the performance of the complete biosensor is governed not only by the intrinsic catalytic activity of the nanozyme but also by complex physicochemical interactions within the immobilized biocatalytic layer.

Several factors may account for this behavior. First, differences in the surface chemistry of Cu and CuAu nanoparticles may influence the adsorption, orientation, and surface coverage of alcohol oxidase molecules, thereby affecting the accessibility of the enzyme active sites and catalytic efficiency. Second, stronger interactions between the enzyme and the nCuAu surface may induce subtle conformational changes or restrict enzyme flexibility, leading to reduced catalytic turnover despite the superior electrocatalytic properties of the underlying nanozyme. Third, the local microenvironment of the immobilized enzyme—including surface charge, hydrophilicity, and polymer organization may influence substrate diffusion, hydrogen peroxide transport, and electron-transfer efficiency at the biointerface. Finally, mass-transport limitations within the immobilized sensing layer may become more pronounced in the nCuAu-based architecture, decreasing the efficiency of coupling between enzymatic hydrogen peroxide generation and its electrochemical reduction.

These findings demonstrate that the analytical performance of enzyme–nanozyme hybrid biosensors cannot be predicted solely from the catalytic activity of the nanomaterial. Instead, biosensor performance results from the synergistic interplay between nanozyme electrocatalysis, enzyme immobilization, interfacial electron transfer, and mass transport within the sensing layer. Therefore, rational optimization of all components of the bioelectrode architecture is essential for achieving maximum analytical performance.

3.2. Development and Optimization of Alcohol Oxidase-Based Ethanol Biosensors

The next stage of the work focused on the development of ethanol biosensors based on alcohol oxidase and nanozyme-modified electrodes. Alcohol oxidase catalyzes the oxidation of ethanol to acetaldehyde accompanied by the formation of hydrogen peroxide according to the reaction (1):

$$\text{Ethanol} + O_2 \rightarrow \text{Acetaldehyde} + H_2O_2 \quad (1)$$

The generated hydrogen peroxide is subsequently reduced at the electrode surface, producing an amperometric signal proportional to ethanol concentration. Because the efficiency of the biosensor strongly depends on enzyme immobilization [11], considerable attention was devoted to optimization of the sensor architecture.

Five different immobilization strategies were investigated, including glutaraldehyde vapor cross-linking, dialysis membrane entrapment, incorporation into ELO matrix, incorporation into ELO/RD1 matrix, and incorporation into M1-2 matrix. The performance of the resulting bioelectrodes was evaluated by chronoamperometric measurements following successive additions of ethanol (Figure 3).

Among the tested immobilization methods, glutaraldehyde cross-linking, dialysis membrane entrapment, and ELO matrix incorporation provided the highest analytical responses. The observed high current signals indicate efficient retention of enzymatic activity and favorable mass transport of substrate and reaction products. In contrast, immobilization within ELO/RD1 and M1-2 matrices resulted in significantly lower responses. This behavior is likely caused by diffusion limitations arising from the denser polymer networks, which restrict substrate accessibility to the enzyme active sites and slow down the transport of reaction products toward the electrode surface.

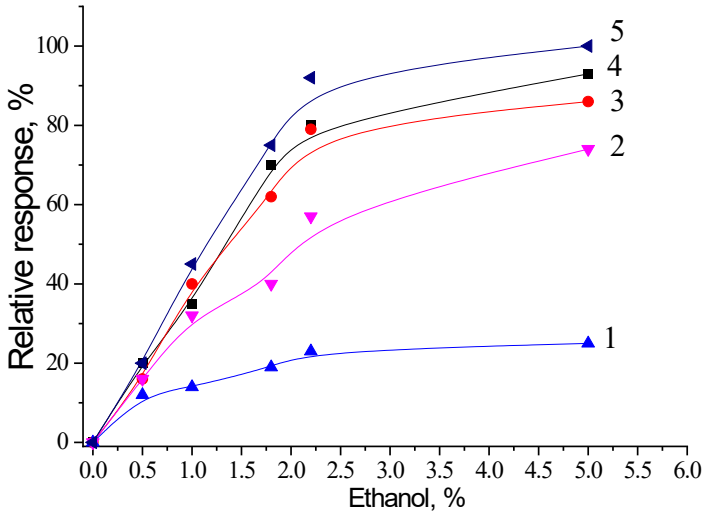

Figure 3. Effect of enzyme immobilization strategy on the analytical performance of AO/nCuAu/GE bioelectrodes. Calibration curves obtained for ethanol determination using alcohol oxidase immobilized by (1) M1-2 matrix entrapment; (2) ELO/RD1 matrix entrapment; (3) ELO matrix entrapment; (4) glutaraldehyde vapor cross-linking; and (5) dialysis membrane coating.

Considering both analytical performance and fabrication simplicity, the ELO matrix was selected for further experiments. The ELO matrix provided stable immobilization while maintaining high catalytic activity of the enzyme–nanozyme complex (Figure 4).

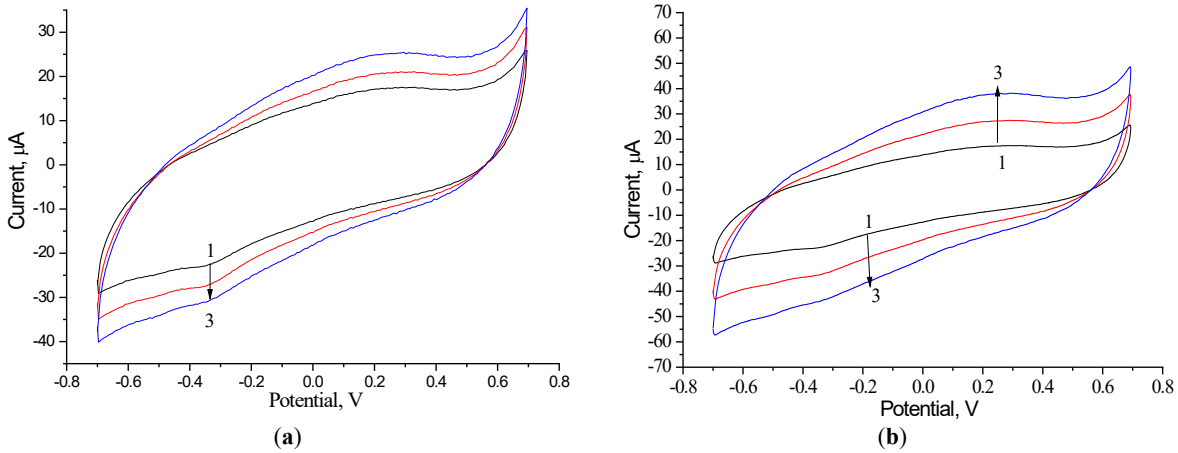

Figure 4. Cyclic voltammetric responses of AO/nCu/GE (**a**) and AO/nCuAu/GE (**b**) bioelectrodes in the presence of increasing ethanol concentrations: 0 mM (1), 2.5 mM (2), and 5.0 mM (3). Measurements were performed at a scan rate of 50 mV·s^{-1} using an Ag/AgCl (3M KCl) reference electrode in 50 mM phosphate buffer (pH 7.5).

The electrochemical behavior of AO/nCu/GE and AO/nCuAu/GE bioelectrodes was investigated using cyclic voltammetry (Figure 4) and chronoamperometry (Figure 5). Upon addition of ethanol, both biosensors exhibited concentration-dependent current responses, confirming successful coupling between enzymatic oxidation and nanozyme-catalyzed hydrogen peroxide reduction.

Detailed analytical characterization revealed noticeable differences between the two sensor architectures. The AO/nCu/GE biosensor exhibited a sensitivity of 95 A·M^{-1}·m^{-2}, whereas the AO/nCuAu/GE biosensor displayed a sensitivity of 35 A·M^{-1}·m^{-2}. The corresponding apparent Michaelis–Menten constants (K_M^{app}) were 19.1 and 37.2 mM, respectively. The lower K_M^{app} value obtained for AO/nCu/GE indicates a stronger apparent affinity toward ethanol and more efficient biocatalytic conversion under the selected experimental conditions.

Interestingly, although nCuAu demonstrated superior catalytic activity toward hydrogen peroxide reduction when tested as a nanozyme alone (Figure 2d–f), the corresponding AO/nCuAu/GE biosensor exhibited lower sensitivity toward ethanol than AO/nCu/GE (Figure 5c,d). This observation suggests that biosensor performance is governed not only by intrinsic nanozyme activity but also by factors such as enzyme orientation, enzyme–nanoparticle interactions, local microenvironment, and diffusion characteristics within the sensing layer. These

results emphasize the importance of optimizing the entire bioelectrode architecture rather than focusing exclusively on the catalytic properties of individual components.

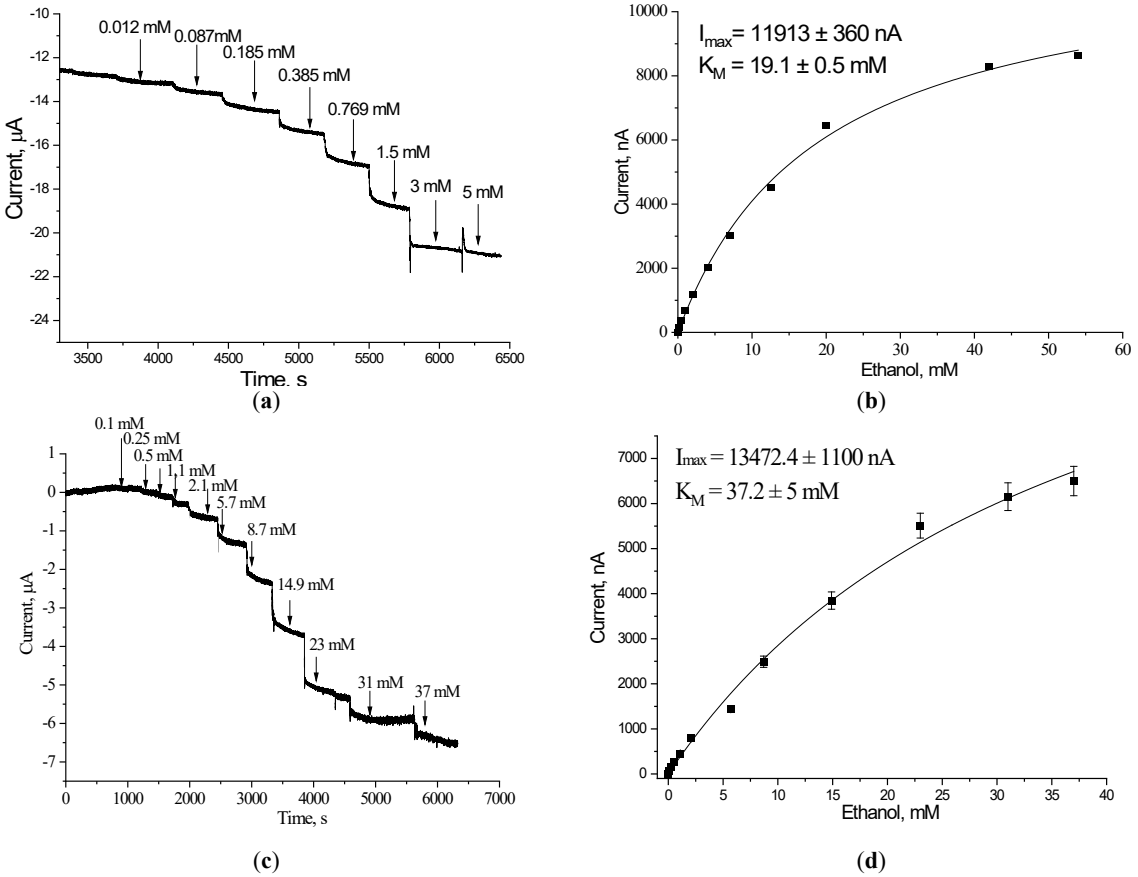

Figure 5. Amperometric characterization of AO/nCu/GE and AO/nCuAu/GE biosensors for ethanol detection. (**a**,**d**) Chronoamperograms recorded following successive additions of ethanol; (**b**,**e**) calibration curves obtained over the entire investigated concentration range; and (**c**,**f**) enlarged views of the linear calibration regions for AO/nCu/GE (**a**–**c**) and AO/nCuAu/GE (**d**–**f**), respectively. Measurements were performed at an applied potential of −200 mV vs. Ag/AgCl (3M KCl) in 50 mM phosphate buffer (pH 7.5).

3.3. Construction and Analytical Performance of the ADH-Based Ethanol Biosensor

In addition to alcohol oxidase-based systems, an alternative ethanol biosensor was developed using alcohol dehydrogenase. In this configuration, ADH together with the $NADP^+$ cofactor was immobilized within the ELO polymer matrix on the graphite electrode surface. Benzoquinone (1 mM) was employed as an electron-transfer mediator to facilitate electrochemical regeneration of the enzymatic system and improve signal transduction.

Cyclic voltammetry demonstrated clear increases in oxidation current after ethanol addition, confirming efficient catalytic conversion of ethanol by the immobilized enzyme (Figure 6a). Based on these studies, an operating potential of +500 mV was selected for chronoamperometric measurements (Figure 6b).

The analytical characteristics of the ADH/ELO/GE biosensor were significantly superior to those of the alcohol oxidase-based systems (Table 1).

Table 1. Analytical performance parameters of the developed alcohol oxidase (AO)- and alcohol dehydrogenase (ADH)-based bionanosensors for ethanol determination.

Electrode Configuration	Applied Potential (mV)	Sensitivity ($A \cdot M^{-1} \cdot m^{-2}$)	Linear Range (mM)	K_M^{app} (mM)	Limit of Detection (mM)
AO/nCuAu/GE	−200	35	0.010–22.0	37.2	0.007
AO/nCu/GE	−200	95	0.20–1.00	19.1	0.15
ADH/ELO/GE	+500	305	0.010–0.14	0.4	0.005

The biosensor exhibited a sensitivity of 305 $A \cdot M^{-1} \cdot m^{-2}$, which was more than three times higher than that of AO/nCu/GE and nearly nine times higher than that of AO/nCuAu/GE. Furthermore, the sensor demonstrated a

low K_M^{app} of 0.4 mM, indicating highly efficient substrate conversion and favorable enzyme kinetics. The linear working range extended from 0.010 to 0.14 mM ethanol, while the limit of detection reached 0.005 mM (Table 1).

Selectivity studies revealed excellent analytical specificity of the developed ADH/ELO/GE biosensor (Figure 7).

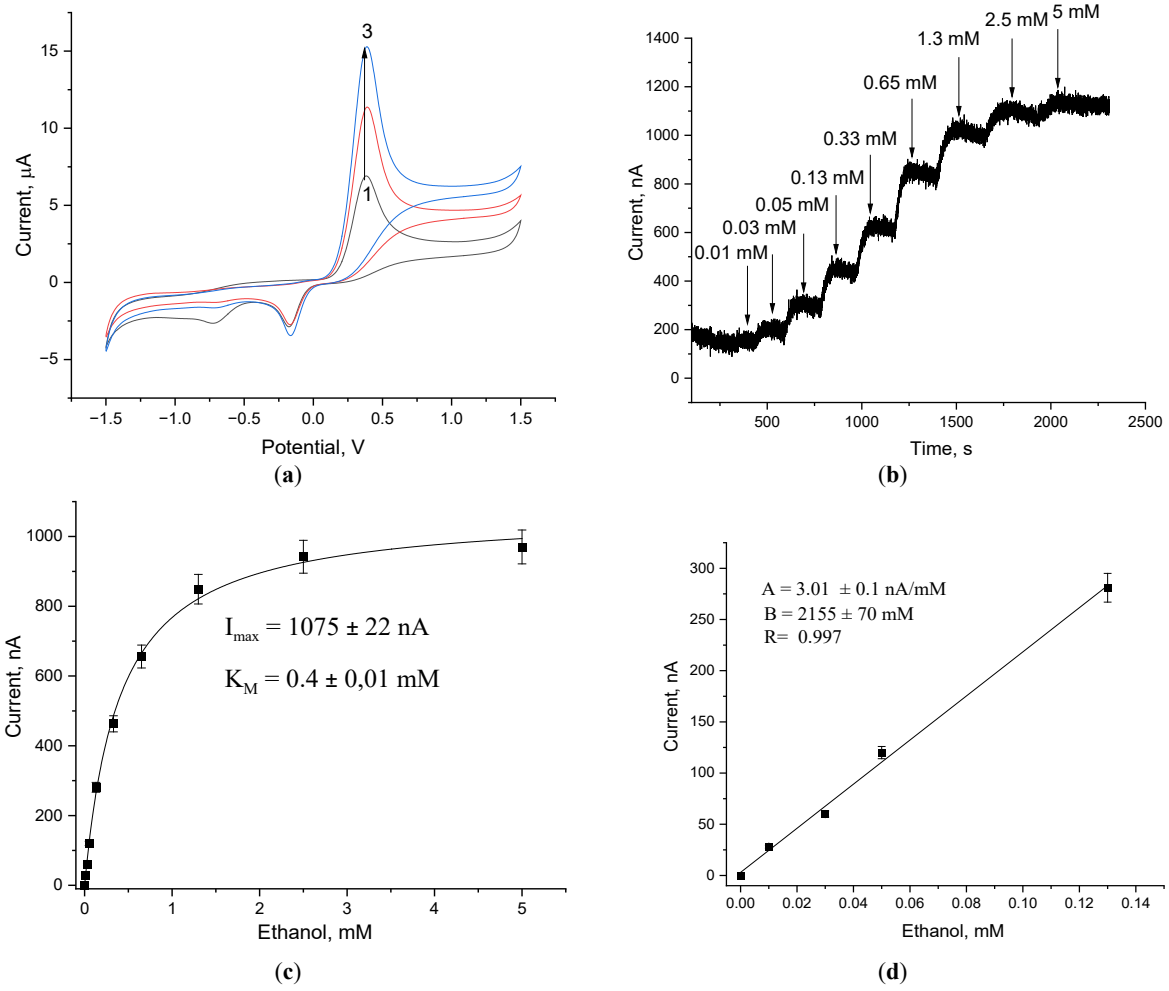

Figure 6. Amperometric characteristics of the ADH/ELO/GE bionanoelectrode for ethanol determination. (**a**) Cyclic voltametric response under the injection of increased concentrations of ethanol: 1–base line; 2–0.08 mM ethanol; 3–0.14 mM ethanol; (**b**) Representative chronoamperometric responses recorded upon successive additions of ethanol; (**c**) calibration curve showing the dependence of amperometric current response on ethanol concentration over the full concentration range; and (**d**) calibration plot within the linear concentration range. Experimental conditions: applied potential of +500 mV vs. Ag/AgCl (3M KCl) in 50 mM phosphate buffer, pH 7.5.

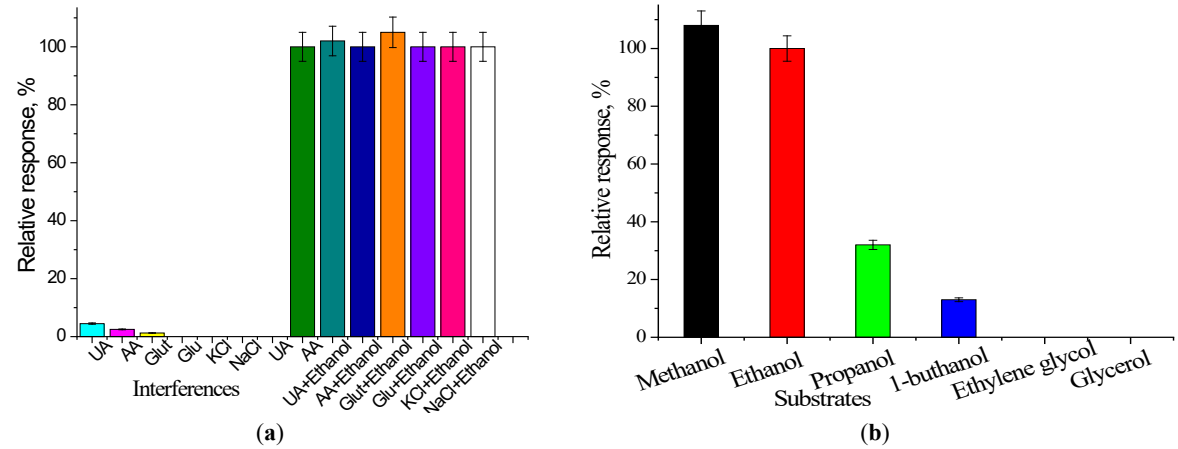

Figure 7. Selectivity studies of the ADH/ELO/GE ethanol bionanosensor. (**a**) Effect of potential interfering compounds (1 mM each) on the sensor response; (**b**) relative responses toward different alcohols (1 mM). Current

signals recorded at an applied potential of −200 mV were normalized to the response obtained for ethanol, which was assigned a value of 100%. Results are presented as relative response percentages. Abbreviations: UA—uric acid; AA—ascorbic acid; Glu—glutamic acid; Glut—glutamine.

Common electroactive compounds present in biological and food samples, including ascorbic acid, uric acid, dopamine, glutathione, sodium chloride, and potassium chloride, produced only negligible interference. The signal changes caused by these compounds remained below 5%, confirming that the developed sensing platform can selectively determine ethanol in complex sample matrices (Figure 7a). Additional experiments were performed to investigate the response toward different alcohols. The ADH/ELO/GE biosensor exhibited its highest response toward ethanol and methanol, whereas significantly lower signals were recorded for propanol, butanol, ethylene glycol, and glycerol (Figure 7b). These results indicate a degree of substrate specificity associated with the catalytic properties of the immobilized alcohol dehydrogenase.

The practical applicability of the ADH/ELO/GE biosensor was evaluated through reproducibility, repeatability, and storage stability studies. Five consecutive measurements of 1.3 mM ethanol performed within a single day resulted in a relative standard deviation of only 3.5%, demonstrating excellent repeatability. Measurements conducted over five consecutive days yielded an RSD of 3.9%, confirming good reproducibility of sensor fabrication and operation.

Storage stability tests revealed gradual loss of activity during long-term storage at 4 °C (Figure 8).

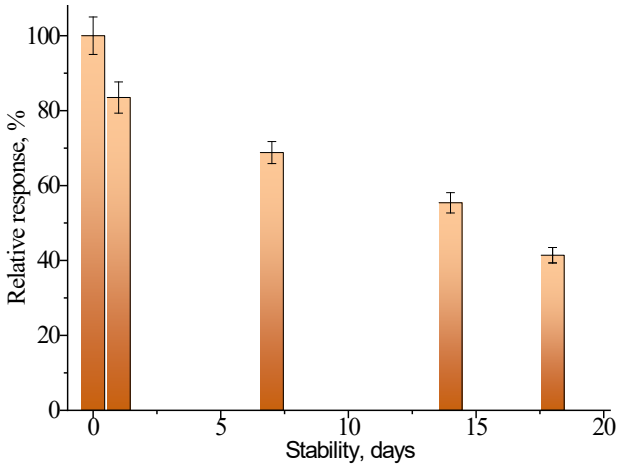

Figure 8. Stability of the ADH/ELO/GE bio-nanoelectrodes during storage at +4 °C.

Nevertheless, approximately 54% of the initial signal was retained after 14 days, indicating acceptable operational stability for laboratory applications. The observed decrease in response is likely associated with gradual enzyme deactivation and structural changes within the immobilized biocatalytic layer. Future improvements in storage stability may be achieved through rational engineering of the immobilization layer. Strategies such as covalent enzyme immobilization, co-entrapment with protein or sugar stabilizers (e.g., bovine serum albumin, trehalose, or glycerol), incorporation of nanostructured protective coatings, and optimization of the polymer microenvironment to preserve enzyme hydration and reduce conformational changes are expected to further prolong the operational lifetime of the biosensor. These approaches will be investigated in our future studies aimed at developing long-term stable analytical platforms.

Finally, the developed ADH/ELO/GE biosensor was applied to the determination of ethanol in commercial "Isabella" red wine. Ethanol concentrations obtained using the biosensor were compared with results provided by a commercial enzymatic assay kit "Alkotest" (Table 2).

Table 2. Determination of ethanol content (%) in "Isabella" red wine.

Tested Sample	Value Declared by Manufacturer	ADH/ELO/GE	Alkotest
"Isabella" wine	11–13%	12.505 ± 0.7%	11.9 ± 0.50%

Note: $p > 0.05$; Student's *t*-test was used to compare results obtained by the biosensor-based method (ADH/ELO/GE) and the "Alkotest" method/kit.

Excellent agreement between the two methods was observed, yielding a correlation coefficient of R = 0.999. The measured ethanol content (12.5 ± 0.7%) was statistically indistinguishable from the reference value (11.9 ± 0.5%), demonstrating the accuracy and practical applicability of the developed biosensor (Table 2). Beyond wine analysis, the proposed biosensor could be extended to the determination of ethanol in beer, cider, distilled beverages, and fermentation broths used in food and biotechnological industries. Its rapid response, high sensitivity, and simple operation make it attractive for routine process monitoring. Nevertheless, complex sample matrices may contain suspended solids, proteins, polyphenols, pigments, sugars, and other electroactive constituents that could affect enzyme activity or the electrochemical response. Therefore, simple sample pretreatment (e.g., dilution, filtration, or centrifugation) together with calibration using the standard addition method may be required for accurate analysis of highly complex samples. Future work will focus on validating the biosensor in a broader range of real fermentation matrices.

Overall, the obtained results demonstrate that although alcohol oxidase-based nanozyme biosensors provide an attractive mediator-free approach, the ADH/ELO/GE platform offers superior analytical performance in terms of sensitivity, detection limit, and practical applicability. The combination of alcohol dehydrogenase, $NADP^+$, benzoquinone mediator, and ELO immobilization matrix constitutes a promising strategy for the development of next-generation electrochemical ethanol biosensors.

4. Conclusions

Copper and copper–gold nanoparticles were successfully synthesized and evaluated as nanozyme-like catalytic materials for ethanol biosensor construction. Optimization of enzyme immobilization demonstrated that the ELO matrix provides efficient retention of enzymatic activity and stable sensor performance. AO-based biosensors showed promising analytical characteristics, particularly when copper nanoparticles were employed. However, the ADH/ELO/GE biosensor exhibited superior sensitivity, lower detection limit, and excellent analytical performance. The developed biosensor demonstrated high selectivity, good reproducibility, acceptable storage stability, and successful application to real sample analysis. These results highlight the potential of enzyme–nanozyme hybrid systems for practical ethanol monitoring in food, clinical, and industrial applications.

Author Contributions

N.S.: investigation, writing original manuscript; O.D.: data curation, software; H.K.: visualization, investigation; T.K.: supervision; J.O.: visualization, investigation; M.G.: writing—reviewing and editing. All authors have read and agreed to the published version of the manuscript.

Funding

This research was financed by the Ministry of Education and Science of Ukraine (projects Nos. 0125U001054, 0125U002005, and 0125U002033), Joint Polish-Ukrainian mobility project for the years 2025–2027 under the agreement on scientific cooperation between the Polish Academy of Sciences and the National Academy of Sciences of Ukraine, National Research Foundation of Ukraine (project No. 2021.01/0010), by the "Presidential Discretionary-Ukraine Support Grants" from the Simons Foundation (Award No 1030281). Nataliya Stasyuk gratefully acknowledges financial support from the Boris Paton Named Scholarship of the Verkhovna Rada of Ukraine for Young Scientists—Doctors of Sciences (2026). This work was also supported in part by the National Research Foundation of Ukraine (project No. 2020.02/0100). Taras Kavetskyy also acknowledges the SAIA (Slovak Academic Information Agency) for a scholarship in the Institute of Physics of the Slovak Academy of Sciences in the framework of the National Scholarship Programme of the Slovak Republic. This work has also received funding through the MSCA4Ukraine project (grant No. 1128327), which is funded by the European Union.

Institutional Review Board Statement

Not applicable.

Informed Consent Statement

Not applicable.

Data Availability Statement

Data is contained within the article.

Conflicts of Interest

The authors declare no conflict of interest.

Use of AI and AI-Assisted Technologies

During the preparation of this work, the authors used ChatGPT for language polishing. After using this tool/service, the authors reviewed and edited the content as needed and take full responsibility for the content of the published article.

References

1. Clark, L.C.; Lyons, C. Electrode Systems for Continuous Monitoring in Cardiovascular Surgery. *Ann. N.Y. Acad. Sci.* **1962**, *102*, 29–45. https://doi.org/10.1111/j.1749-6632.1962.tb13623.x.
2. Smutok, O.; Katz, E. *Bioelectrochemistry* & *Biosensors*—Inaugural Issue: In Memory of Leland Charles Clark—"Father" of Biosensors. *Bioelectrochem. Biosens.* **2026**, *1*, 1. https://doi.org/10.53941/bebs.2026.100001.
3. Turner, A.P.F. Biosensors: Sense and Sensibility. *Chem. Soc. Rev.* **2013**, *42*, 3184–3196. https://doi.org/10.1039/c3cs35528d
4. Updike, S.J.; Hicks, G.P. The Enzyme Electrode. *Nature* **1967**, *214*, 986–988. https://doi.org/10.1038/214986a0.
5. Campuzano, S.; Yáñez-Sedeño, P.; Pingarrón, J.M. Electrochemical Biosensing of NADH/NAD^+ Systems. *Biosens. Bioelectron.* **2021**, *181*, 113133. https://doi.org/10.1016/j.bios.2021.113133.
6. Stasyuk, N.; Smutok, O.; Demkiv, O.; et al. Synthesis, Catalytic Properties and Application in Biosensorics of Nanozymes and Electronanocatalysts: A Review. *Sensors* **2020**, *20*, 4509. https://doi.org/10.3390/s20164509.
7. Huang, Y.; Zhong, H.; Jiang, C.; et al. Copper-Based Nanomaterials as Peroxidase Candidates for Intelligent Colorimetric Detection and Antibacterial Applications. *Particuology* **2024**, *84*, 126–135. https://doi.org/10.1016/j.partic.2023.03.009.
8. Abdel-Mageed, H.M. Frontiers in Nanoparticles Redefining Enzyme Immobilization: A Review Addressing Challenges, Innovations, and Unlocking Sustainable Future Potentials. *Micro Nano Syst. Lett.* **2025**, *13*, 7. https://doi.org/10.1186/s40486-025-00228-2.
9. Smutok, O.; Kavetskyy, T.; Prokopiv, T.; et al. New Micro/Nanocomposite with Peroxidase-Like Activity in Construction of Oxidases-Based Amperometric Biosensors for Ethanol and Glucose Analysis. *Anal. Chim. Acta* **2021**, *1143*, 201–209. https://doi.org/10.1016/j.aca.2020.11.052.
10. Andersen, J.E.T. The Standard Addition Method Revisited. *TrAC Trends Anal. Chem.* **2017**, *89*, 21–33. https://doi.org/10.1016/j.trac.2016.12.013.
11. Kavetskyy, T. Impact of Polymer Microstructure and Free Volume on Electrochemical Biosensor Functionality. *Bioelectrochem. Biosens.* **2026**, *1*, 7. https://doi.org/10.53941/bebs.2026.100007.